RESEARCH Open Access



PHPT1 acts as an inhibitor in high-altitude pulmonary hypertension via negative TRPV5 signaling regulation

Ge Guo^{1†}, Ming-xiang Zhu^{2†}, Xiang Xu¹, Xin Li¹, Yi-bing Chen¹, Yan-ying Shen¹, Han-lu Li¹, Li-ting Cheng², Kun-lun He^{1,2*}, Yong-ming Yao^{1,3*} and Chun-lei Liu^{1*}

Abstract

Background Low barometric pressure hypoxia at high altitudes triggers vascular remodeling, resulting in high-altitude pulmonary hypertension (HAPH). The key step is the transformation of pulmonary artery smooth muscle cells (PASMCs) from a contractile to synthetic phenotype. Protein kinases and phosphatases contribute to phenotype transformation by altering phosphorylated protein expression.

Objectives In this study, we aimed to investigate the role of phosphohistidine phosphatase 1 (PHPT1) in PASMC transformation and its regulatory pathway in HAPH.

Methods An HAPH model was constructed in wild-type, PHPT1⁻/⁻, and PHPT1⁺/⁺ rats by placing them in a hypobaric chamber. Evaluations included hemodynamic measurements, echocardiography, histopathological analysis, and various cellular assays. RNA-seq and western blotting were used to identify intervention targets, and co-immunoprecipitation was used to determine the interaction between PHPT1 and TRPV5.

Results PHPT1 protein expression was downregulated in HAPH, and its knockdown impaired cardiopulmonary functions, including elevated mean pulmonary artery pressure (mPAP), right ventricular systolic pressure (RVSP), and increased right ventricular thickness, and enhanced PASMC proliferation and migration. PHPT1 directly interacted with TRPV5 phosphorylation sites, whereas Asp30Ala/Arg157Ala functioned to prevent this interaction. PHPT1 overexpression protected against cardiopulmonary damage, reducing mPAP, RVSP, the D/W ratio, and MWT%. Additionally, PHPT1 overexpression mitigated PASMC proliferation and migration, resulting in restored TRPV5, p-Akt, p-SMAD2/3, and p-TGF-β expression under hypoxic conditions.

[†]Ge Guo and Ming-xiang Zhu have contributed equally to this work as co-first authors.

*Correspondence: Kun-lun He kunlunhe@plagh.org Yong-ming Yao c_ff@sina.com Chun-lei Liu chunleiliu87@163.com

Full list of author information is available at the end of the article



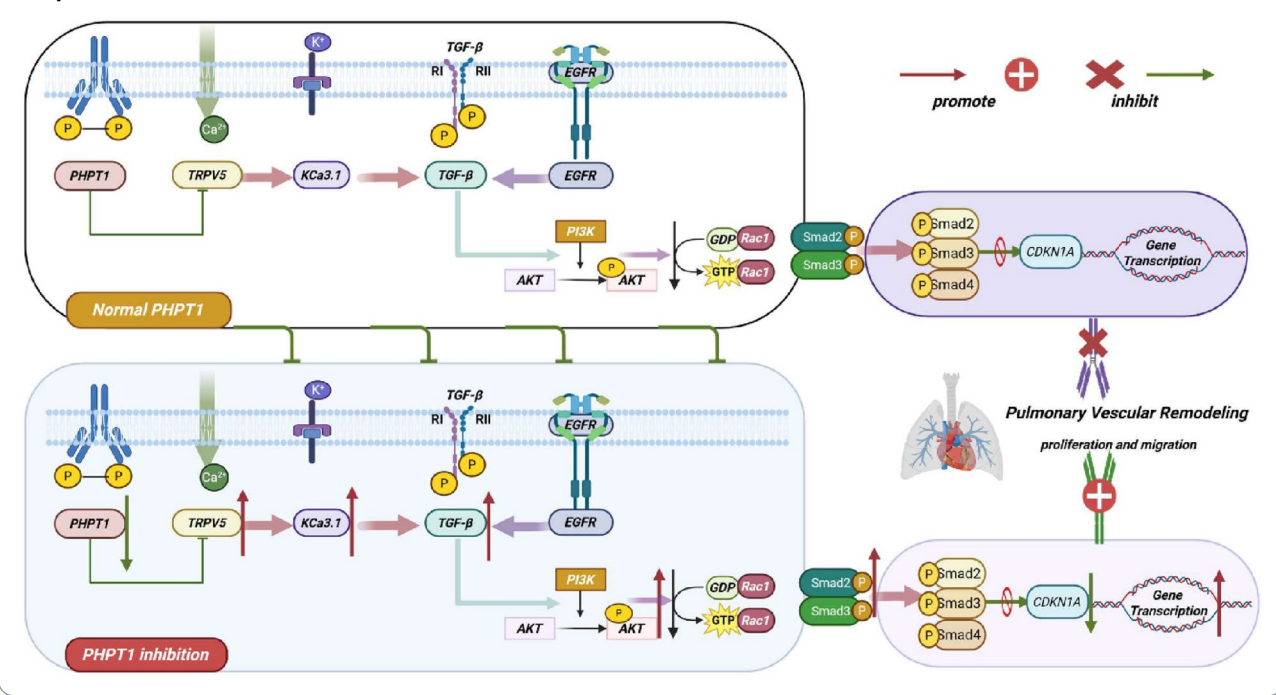
© The Author(s) 2025. **Open Access** This article is licensed under a Creative Commons Attribution-NonCommercial-NoDerivatives 4.0 International License, which permits any non-commercial use, sharing, distribution and reproduction in any medium or format, as long as you give appropriate credit to the original author(s) and the source, provide a link to the Creative Commons licence, and indicate if you modified the licensed material. You do not have permission under this licence to share adapted material derived from this article or parts of it. The images or other third party material in this article are included in the article's Creative Commons licence, unless indicated otherwise in a credit line to the material. If material is not included in the article's Creative Commons licence and your intended use is not permitted by statutory regulation or exceeds the permitted use, you will need to obtain permission directly from the copyright holder. To view a copy of this licence, visit http://creativecommons.org/licenses/by-nc-nd/4.0/.

Guo et al. Journal of Translational Medicine (2025) 23:968 Page 2 of 19

Conclusions These findings underscore that PHPT1 inhibits PASMC proliferation and migration through TRPV5 signaling, thereby reducing mPAP and improving right ventricular function in HAPH. Therefore, PHPT1 targeting could potentially contribute to the development of novel therapeutic approaches for treating HAPH.

Keywords PHPT1, High-altitude pulmonary hypertension, TRPV5 signaling, Ca²⁺ signaling

Graphical abstract



Introduction

More than 80 million people worldwide permanently live in high-altitude areas (i.e., >2500 m), and more than 40 million people visit these areas annually, exposing themselves to chronic hypobaric hypoxia [1]. At altitudes >2500 m, the barometric pressure is low, and the actual amount of oxygen reaching the alveoli is lower than that at sea level, thereby leading to hypoxia. Hypoxia triggers abnormal smooth muscle production, vascular remodeling, and, ultimately, increased pulmonary artery pressure [2]. The transformation of pulmonary artery smooth muscle cells (PASMCs) from a contractile to a synthetic phenotype is considered a key step in vascular remodeling during the development of high-altitude pulmonary hypertension (HAPH) [3].

Phosphorylation is believed to play a key role in the development of pulmonary arterial hypertension (PAH) and has also been implicated in regulating the phenotypic transformation of PASMCs [4]. Protein phosphatases catalyze the dephosphorylation of phosphorylated proteins. They work in tandem with protein kinases to form a phosphorylation and dephosphorylation switching system [5]. We previously investigated the impact of low oxygen at high altitudes on differentially expressed histidine phosphatases; the expression of phosphohistidine

phosphatase 1 (PHPT1), was approximately 20-fold lower than that of the normal group [6]. PHPT1 encodes an enzyme that catalyzes the reversible dephosphorylation of histidine proteins. Notably, PHPT1 is primarily distributed in the heart, skeletal muscle, lung, and other tissues and has been previously proven to be associated with pulmonary diseases, consistent with the expression of cell proliferation or apoptosis regulatory factors [7]. Furthermore, PHPT1 has been implicated in lung cancer cell migration by mediating TGF- β 1 signaling through the PI3K γ /Akt/Rac1 pathway [8]. FBXO32 targets PHPT1 for ubiquitination to regulate the growth of EGFR mutant lung cancer [9]. Nevertheless, the potential involvement of PHPT1 in the development of HAPH remains largely unclear.

In the present study, we sought to elucidate the possible role and underlying mechanisms in high-altitude-induced pulmonary hypertension. We identified a novel molecular mechanism underlying the action of the PHPT1-TRPV5-Akt pathway in alleviating HAPH. TRPV5 and Akt inhibition significantly mitigated HAPH severity under hypobaric hypoxic conditions. Specifically, PHPT1 inhibition induced Ca²⁺ misalignment by upregulating TRPV5 phosphorylation, subsequently dysregulating spontaneous Ca²⁺ events and Ca²⁺ current.

Our findings provide the first mechanistic basis for PHPT1-derived TRPV5 alleviation of HAPH and identify a promising target for treating this complication at high altitudes.

Materials and methods

Reagents

The reagents were described in Table S1.

Animals

Sprague-Dawley rats (250-300 g) were provided by the Animal Experiment Center of the People's Liberation Army (PLA) General Hospital. PHPT1 conditional overexpression (PHPT1-OE) PASMC and PHPT1 conditional knockdown (PHPT1-KD) rat models were generated by Biocytogen Pharmaceuticals Ltd. (Beijing, China) using the Biocytogen Extreme Genome Editing System. The primers for identifying rat DNA were designed and used accordingly, and their sequences are provided in Table S2. Animal experiments were approved by the PLA General Hospital Animal Ethics Committee and performed in accordance with NIH guidelines for laboratory animal care and use (Approval ID: 2020-X16-01). Control rats were housed in a normoxic environment (n = 12). To simulate an altitude of 5500 m, the animals in the hypoxia-induced pulmonary hypertension group were kept in a hypobaric chamber (380 mmHg) for 4 weeks (n = 12) .The rats of both sexes were included and the time or dose choices of hypoxia followed the previously experiment [10].

Echocardiography

Rats were anesthetized with isoflurane gas and then placed in a supine position on a heated platform with electrodes attached to all four limbs for heart rate monitoring. Transthoracic echocardiography was conducted using the Vevo 2100 system with a 30-MHz transducer (VisualSonics, Canada), measuring tricuspid annular plane systolic excursion (TAPSE) and pulmonary acceleration time/pulmonary ejection time (PAT/PET).

Hemodynamic measurement

After hypoxia exposure, rats were tracheotomized and received breathing assistance through a rodent ventilator (Kent Scientific, Torrington, CT, USA). A Millar SPR-838 pressure-volume catheter (ADInstruments, Colorado Springs, CO, USA) was inserted into the right ventricle and subsequently advanced into the pulmonary artery. Pressure measurements were performed using the MPVS Ultra system in conjunction with a PowerLab data acquisition system (ADInstruments, Colorado Springs, CO, USA), followed by right ventricular systolic pressure (RVSP) and mean pulmonary artery pressure (mPAP) estimation.

Tissue sampling and histopathological analysis

The animals were euthanized and immediately dissected. The chest cavity was opened, the lung tissue was removed, and its total weight was recorded. Next, the lung tissue was placed in an oven and dried completely for 72 h at 160 °C. The dry and wet weight ratio was then calculated to determine pulmonary edema severity. The right ventricular hypertrophy index (RVHI) was calculated as the ratio of the right ventricular weight to the combined weight of the left ventricle and septum (RV/LV + IS). Hearts and right lung tissues were snapfrozen in liquid nitrogen. Further fresh heart and upper left lung tissues were fixed with 4% paraformaldehyde for hematoxylin and eosin (H&E), Masson, and immunofluorescence staining. Immunofluorescence staining was performed on lung sections using proliferating cell nuclear antigen (PCNA)-specific and anti-α-SMA primary antibodies to evaluate PASMC proliferation in vivo. ProLong Gold Antifade reagent with DAPI (4',6-diamidino-2-phenylindole; Invitrogen, Carlsbad, CA, USA) was used to mount and counterstain the slides. The shortest external diameter (2 × wall thickness/external diameter), with the average thickness, was described as the mean wall thickness (MWT). All images were analyzed using the ImageJ software (Washington, DC, USA).

Cell culture

PASMCs were maintained in Dulbecco's Modified Eagle Medium (DMEM) supplemented with 10% fetal bovine serum (FBS). For hypoxia-related studies, the cells were cultured in a cell precision control system (AVATAR, Xcellbio, USA) at 37 °C with 5 % CO₂ and 1% oxygen for 24 h. Lentiviral vectors, constructed by Jikai Gene Chemical Technology Ltd. (Shanghai, China), were used to overexpress or knock down PHPT1. PHPT1 overexpression, knockdown, and negative control lentiviruses were titrated at 10⁸ transfection units per milliliter. TRPV5 mutant (Arg157Ala and Asp30Ala)-encoding plasmids were generated and transfected using Lipofectamine 3000 (Invitrogen, Carlsbad, CA, USA) according to the manufacturer's protocol. Cells were collected 48–72 h post-transfection for subsequent analyses.

Cell proliferation and migration assays

For proliferation assessment, basal cell impedance was continuously recorded using a Nanion CardioExcyte 96 electrophysiological detector (Nanion Technologies, Munich, Germany). Cells were seeded in 96-well plates, and their impedance values were recorded. Moreover, cell proliferation was evaluated using a CCK8 assay (Dojindo Laboratories, Shanghai, China). Cell migration was assessed using a scratch assay, making straight scratches with a 200- μ L pipette tip. Transwell chambers (pore size: 8 μ m, Corning Inc., Corning, NY, USA) were

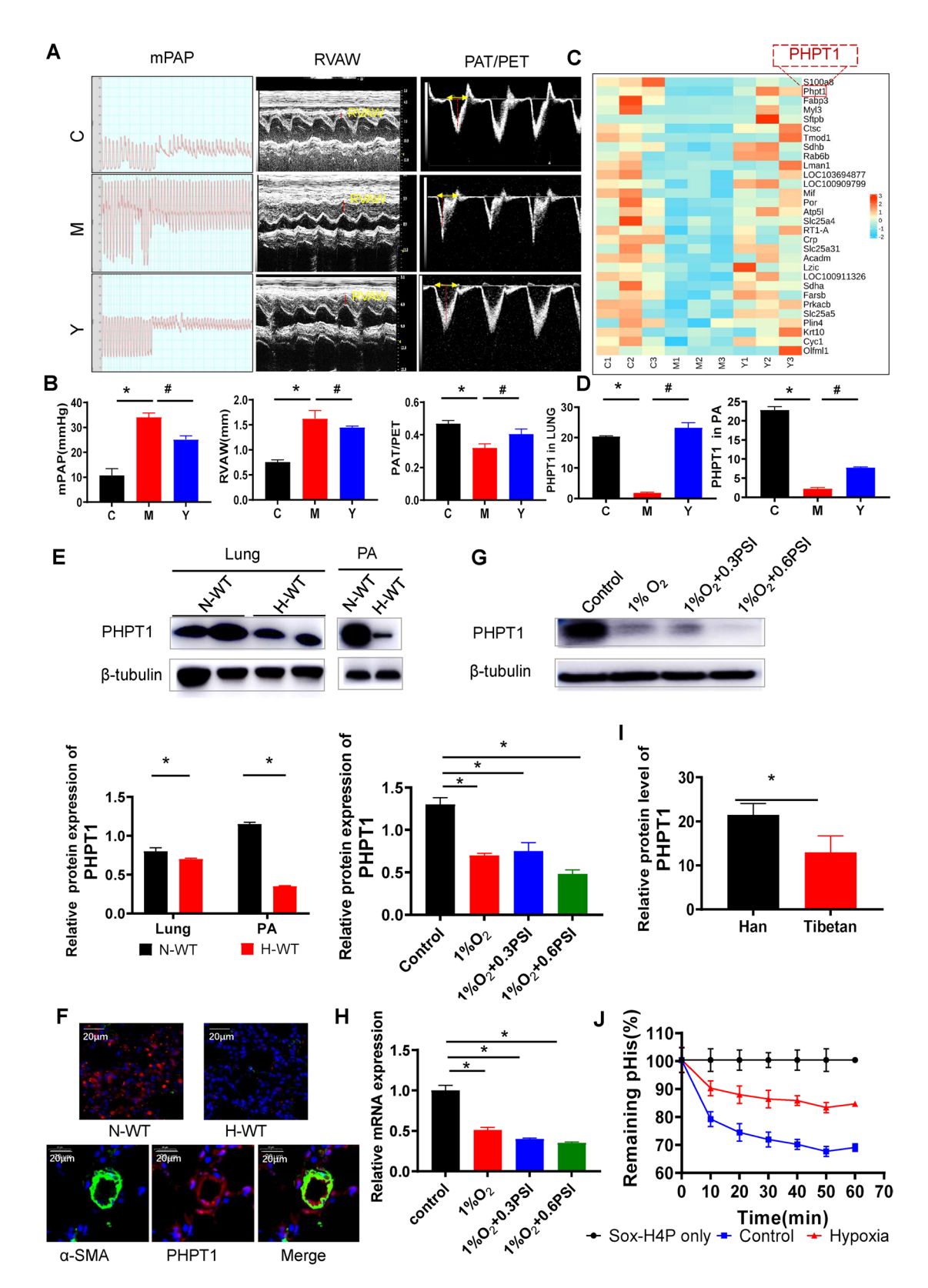


Fig. 1 (See legend on next page.)

Fig. 1 PHPT1 is downregulated in the lungs and pulmonary arteries in HAPH rats. A Cardiac hemodynamics and ultrasonic images of the control (C), hypoxia model (M), and macititan treatment groups (Y) of a rat HPH model. B mPAP, RVAW, and PAT/PET level quantifications (n = 12). C Heatmap presenting DEG downregulation during hypoxia and drug treatment-induced reversal. D PHPT1 level quantification in the lungs and pulmonary arteries (n = 12). E PHPT1 expression level in the lungs and pulmonary arteries of HAPH rats assessed by western blotting. F Pulmonary rat lung sections both from the control and HAPH groups. Sections were immunostained with antibodies against α-SMA and PHPT1. DAPI was used to stain nuclei. G PHPT1 protein expression levels in hypoxic PASMCs assessed by western blotting. H PHPT1 mRNA expression levels in hypoxic PASMCs determined by RT-qPCR. I PHPT1 levels in Tibetan individuals compared with those in the Han population measured using a proteomics assay. H PHPT1 enzyme activity in hypoxic PASMCs was assessed using the phosphatase probe Sox-H4P. HAPH, high-altitude pulmonary hypertension; PASMCs, pulmonary artery smooth muscle cells; DEG, differentially expressed gene; mPAP, mean pulmonary artery pressure; RVAW, right ventricular anterior wall; PAT/PET, pulmonary acceleration time/pulmonary ejection time. *p < 0.05 relative to control. #p < 0.05 relative to the hypoxia model group.

used for migration analysis. PASMCs were seeded in the upper chambers in a 0.5% FBS-containing medium, while the lower chambers in 24-well plates contained medium with 10% FBS. After 24 h of incubation, the cells on the lower membrane surface were fixed in 4% paraformal-dehyde and stained with crystal violet (Solarbio, China). Subsequently, the cells were resuspended in DMSO, and the absorbance was measured at 590 nm using a microplate reader (Thermo Fisher).

Real-time PCR

The rat heart or lung samples and PASMC were used for real-time PCR evaluations. Total RNA was isolated using the TRIzol reagent, and the DNase-treated RNA was reverse-transcribed using the PrimeScript RT Reagent Kit (Takara Bio Inc., Shiga, Japan). Real-time quantitative PCR was performed with SYBR Premix Ex Taq II (Takara Bio Inc., Shiga, Japan). The target gene Ct values were normalized against the housekeeping gene actin. Relative mRNA expression was calculated using the $2^-\Delta\Delta Ct$ method, setting the control sample mean as 1. Gene specific primers, whose sequences are listed in Table S3.

Western blotting

The rat heart or lung samples and PASMC were subjected to western blotting. The rat tissue samples were homogenized in liquid nitrogen and lysed on ice for 30 min in RIPA buffer (Applygen Technologies, Beijing, China) supplemented with protease and phosphatase inhibitors. For the cell samples, protein lysis was performed directly in RIPA buffer on ice for 1 h. Next, 15-30 µg total protein-containing samples were loaded onto a 10% SDS-PAGE gel. The following primary antibodies were used at specified dilutions as follows: anti-PHPT1 (1:1000, ProteinTech, China), anti-GAPDH (1:2000 Servicebio, China), anti-β tubulin (1:2000, ProteinTech, China), anti-SMA (1:1000 CST, USA), anti-CDKN1A (1:1000, ProteinTech, China), anti-Rac1/Cdc42 (1:1000, CST, USA), anti-KCNN4/KCa3.1 (1:1000, LSBio, USA), anti-Smad3 (1:1000, CST, USA), anti-p-Smad3(1:1000, CST, USA), anti-Smad2 (1:1000, CST, USA), anti-p-Smad2 (1:1000, CST, USA), anti-Akt (1:1000, ProteinTech, China), antip-Akt (1:1000, ProteinTech, China), anti-TRPV5(1:1000, Boster Bio, Pleasanton, CA, USA), anti-TGF-βR II (1:1000, CST, USA), anti-p-TGF- β R II (1:10000, Abcam, United Kingdom), anti-EGFR (1:1000, CST, USA), and anti-p-EGFR (1:1000, CST, USA). HRP-conjugated goat anti-rabbit and goat anti-mouse were used as secondary antibodies (Servicebio, China), visualizing the protein bands with pre-stained protein ladders (Thermo Fisher Scientific, United Kingdom) for molecular weight estimation.

Co-immunoprecipitation (Co-IP)

The cells were lysed in enhanced RIPA buffer containing protease and phosphatase inhibitors. A total of 1 mg of cellular protein was incubated with 10 μg of agarose-conjugated primary antibody (PHPT1 Antibody, Santa Cruz Biotechnology, Dallas, TX, USA) at 4 °C for 1 h with rotation. Immunocomplexes were collected by centrifugation and washed thrice with PBS (pH 7.4). Bound protein samples were eluted by boiling in 2× loading buffer at 95 °C for 5 min and analyzed by SDS-PAGE and western blotting.

Capillary isoelectric focusing

Four micrograms of protein were prepared in RIPA buffer for capillary isoelectric focusing using the Nanopro-1000 system (ProteinSimple, Santa Clara, CA) according to the manufacturer's instructions. Proteins were focused for 40 min at 60 mW, crosslinked to the capillary for 90 s, and then incubated sequentially with primary (1:50) and secondary (1:100) antibodies for 120 and 60 min, respectively. The results are represented as the relative chemiluminescence intensity plotted against pI values, with distances converted into pI values using internal fluorescent standards. Reproducibility was confirmed with a pI variation below 0.05 units among the replicates.

Potassium ion channel detection in PASMCs

Suspensions of PASMC cells were prepared at a concentration of $1\times 10^6 - 5\times 10^7$ cells/mL. Approximately $10-15~\mu L$ of this suspension was placed in the cell chamber of a patch-clamp system, where electrode chips of $2-3.5~M\Omega$ were used. Proper cell sealing and membrane rupture were confirmed by assessing capacitance (Cs $\geq 4~pF$) and series resistance (Rs $\leq 20~M\Omega$). Calcium ion channel data were recorded following the initiation of the experiment.

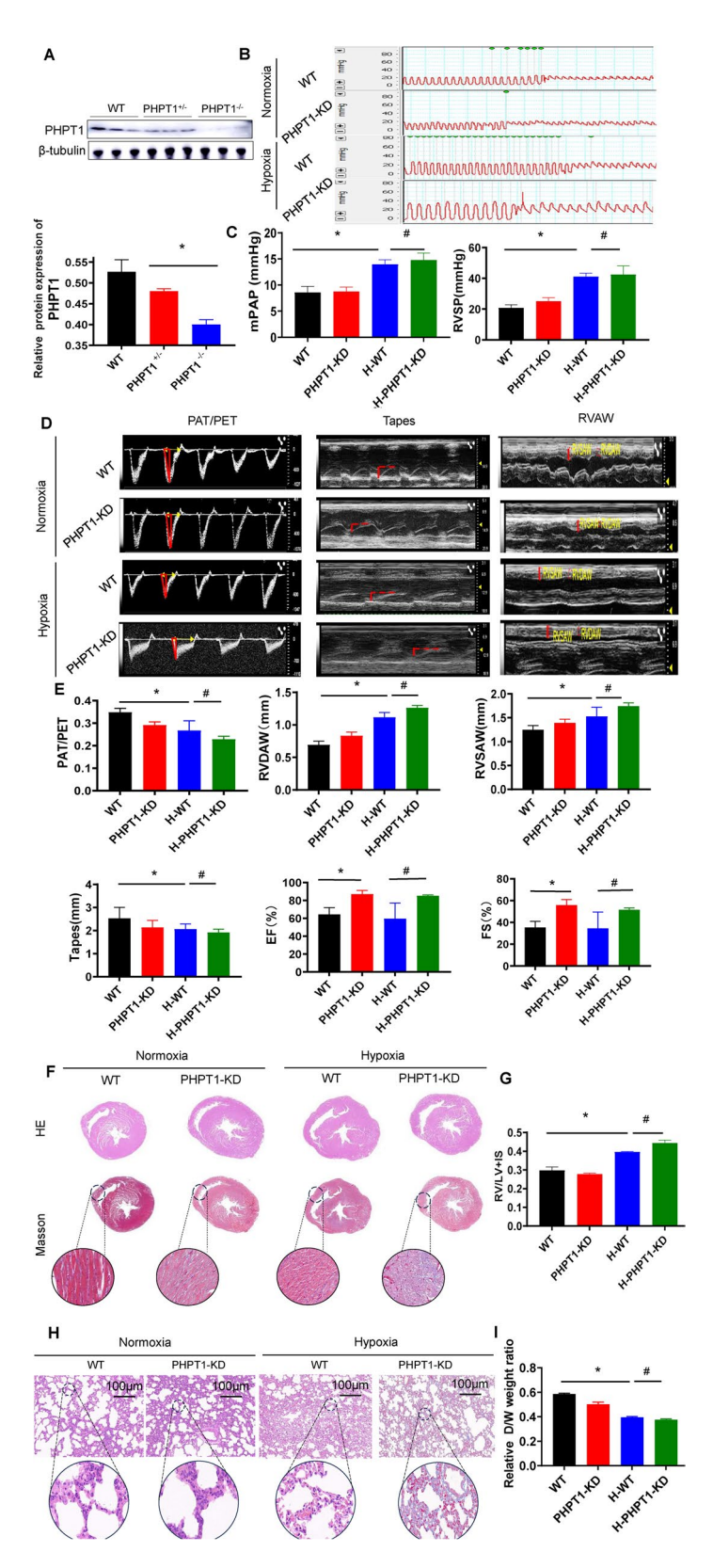


Fig. 2 (See legend on next page.)

Fig. 2 PHPT1 deficiency exacerbates pulmonary vascular remodeling and aggravates HAPH in hypobaric hypoxia rats. A Upper panel: Western blot analysis of PHPT1 protein expression in the lung tissue samples. Tubulin was used as a loading control. Lower panel: Quantification of the western blot analysis from the upper panel. B Cardiac hemodynamics images of the control, PHPT1-KD, hypoxia model, and hypoxia model with PHPT1-KD groups. C) mPAP and RVSP quantification (n = 12). D Cardiac ultrasonic images of the control, PHPT1-KD, hypoxia model, and hypoxia model with PHPT1-KD groups. E PAT/ PET, RVDAW, RVSAW, TAPSE, EF, and FS determined by echocardiography. F Images of heart tissue samples stained with hematoxylin and eosin (H&E) and Masson's staining. G RV to LV+IS ratio quantification (n = 12). H Microscopic images of lung tissue samples stained with H&E. Scale bar: 100 μ m. I Lung dry-to-wet weight ratio. The results are represented as the mean \pm SD (n = 12). KD, knockdown; mPAP, mean pulmonary artery pressure; RVSP, right ventricular systolic pressure; PAT/PET, pulmonary acceleration time/pulmonary ejection time; RVDAW, right ventricular diastolic annular wall; RVSAW, right ventricular to left ventricular + interventricular septum ratio. *p < 0.05 relative to the control. #p < 0.05 relative to the hypoxia model group

Cellular calcium ion concentration detection

Cells were seeded at a density of 1×10^5 cells per well in six-well plates. Fluo-4 AM fluorescent dye (Thermo Fisher Scientific, USA) was prepared by dissolving 50 µg of dye in 22 µL of F127 helper dye (Biotium Corp., Fremont, CA, USA), with 1 µL Fluo-4 AM added to 1 mL hanks solution to create a working solution. Cells were washed twice with PBS (pH 7.4) before being supplemented with the Fluo-4 AM solution and incubated for 45 min in the dark. After removing the dye solution, cells were rinsed twice with hanks solution, and fluorescence intensity was detected under a microscope (SpectraMax M3, Molecular Devices, USA) at 495 nm excitation.

RNA-seq and analysis

Total mRNA was extracted from frozen rat lung tissues, sequenced, and analyzed by RiboBio (Guangzhou, China) using an Illumina HiSeq3000. Briefly, RNA integrity was assessed using an Agilent 2200 TapeStation, and only samples with RINe >7.0. mRNAs were fragmented to approximately 200 bp, converted to cDNA, and prepared for sequencing using the TruSeq RNA LT/HT Sample Prep Kit (Illumina, San Diego, CA, USA). Library quality control was performed with the Agilent 2200 TapeStation, Qubit 2.0, and sequencing was conducted on a HiSeq3000. Raw data were deposited in the Gene Expression Omnibus database (accession no: CRA017617). Bioinformatics analysis was performed using the OmicShare tools (www.omicshare.com/tools).

Statistical analysis

Data are represented as the mean \pm standard deviation (SD). Statistical significance was assessed using an unpaired two-tailed Student's t-test for comparisons between two groups, and the provided data were normally distributed. For comparisons among three or more groups, one-way analysis of variance (ANOVA) followed by the Bonferroni multiple comparison test or Kruskal–Wallis test or two-way ANOVA with Bonferroni's post hoc analysis was performed as appropriate. Data were analyzed using GraphPad Prism version 5.0, considering p-values of p < 0.05 statistically significant.

Results

PHPT1 is downregulated in lungs and pulmonary arteries in HAPH

As shown in Fig. 1A and B, the mean pulmonary artery pressure (mPAP) and right ventricular anterior wall (RVAW) increased in the model and recovered in the treatment group. Contrastingly, pulmonary acceleration time/pulmonary ejection time (PAT/PET) decreased in the model and recovered in the treatment group. We isolated the lung and pulmonary arteries from the rats and applied a fast-seq proteomic workflow. We identified differentially expressed genes (DEGs) and found that PHPT1 was significantly downregulated during hypoxia and could be rescued by treatment (Fig. 1C). PHPT1 expression in the lung and pulmonary arteries is shown in Fig. 1D. We further examined PHPT1 protein transcription levels using western blotting analyses and revealed a significant reduction in PHPT1 expression in HAPH models compared with that in the control group (Fig. 1E). Immunofluorescence staining of rat lung tissue showed that PHPT1 protein colocalized with pulmonary artery smooth muscle and displayed lower expression in the hypoxia group (Fig. 1F). Isolated PASMCs treated with low oxygen and pressure showed a similar decrease in PHPT1 expression through RT-qPCR and western blotting (Fig. 1G and H). In addition, we determined that the PHPT1 expression in the peripheral blood of Tibetan individuals permanently residing at high altitudes was lower than that in the Han population (Fig. 11). Using the small-molecule phosphatase probe Sox-H4P, which selectively targets p-His phosphatases, we found that the level of the remaining p-His was higher in the hypoxia group than in the controls (Fig. 1J). The above data indicate that PHPT1 decreased in lung and pulmonary arteries of HAPH, and might play a vital role in HAPH disease.

PHPT1-KD impairs cardiopulmonary function and aggravates HAPH in hypobaric hypoxia

Based on our observation of decreased PHPT1 expression in HAPH models, we hypothesized that PHPT1 deficiency might contribute to HAPH pathogenesis. To test this hypothesis, we utilized CRISPR/Cas9 technology to generate PHPT1 gene knockdown rats, as depicted in Fig. S1. Protein expression in PHPT1-KD rats was

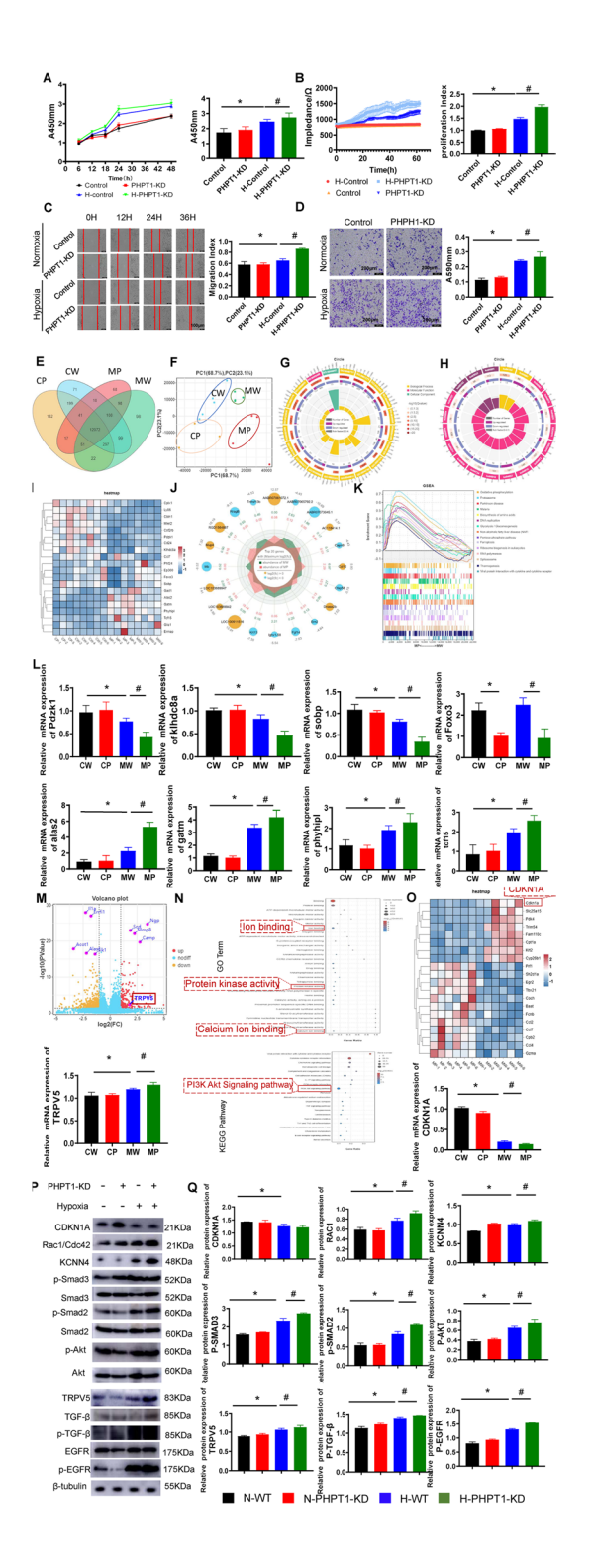


Fig. 3 PHPT1-knockdown results in cardiopulmonary injury by disrupting ion binding and the PI3K/Akt pathway. A Left: Cell proliferation determination using a cell counting kit-8 (CCK-8) under normoxic or hypoxic (1 % O₂) conditions with or without PHPT1 KD, and absorbance measured at 450 nm. Right: CCK8 analysis quantification (n = 6). **B** Left: Cell proliferation determination using impedance detection under normoxic or hypoxic conditions with or without PHPT1 KD. Right: Impedance analysis quantification (n = 6). $\bf C$ Left: PASMCs were exposed to normoxic or hypoxic (1 % O₂) conditions with or without PHPT1 KD for 48 h. Right: Representative images of the wound closure area (scale bars, 50 µm). Right: Wound closure area quantification (n = 6). **D** Left: PASMCs were seeded into the upper chamber of transwell plates and exposed to normoxic or hypoxic (1 % O₂) conditions with or without PHPT1 KD for 48 h. Right: Representative images of the migrated cells (scale bars, 500 µm). Right: The migrated cells were quantified by detecting crystal violet levels (n = 6). **E** Venn diagram of DEGs between WT and PHPT1-KD rat lung samples with or without hypoxia. F PCoA using the Bray-Curtis distance calculated based on the relative abundance of species. The 95% confidence ellipses are shown by circles. **G** Results of GO analysis. **H** Results of KEGG analysis. The significant KEGG sets in environmental information processing, organismal systems and human disease. I Heatmap showing the DEGs among CW, CP, MW and MP groups. J Top 20 genes with maximum abundance of MW or MP. K Results of GSEA analysis. L PCR verification of the RNA-seg results. M Up: Volcano plots of DEGs between WT and PHPT1-KD rat lungs; TRPV5 was significantly increased. Down: PCR verification of the RNA-seq results of TRPV5. ${\bf N}$ Up: Gene Ontology assignment of DEGs between WT and PHPT1-KD rat lungs exposed to hypoxia. Down: Kyoto Encyclopedia of Genes and Genomes pathway enrichment of DEGs between WT and PHPT1-KD rat lungs exposed to hypoxia. O Up: Heatmap showing the DEGs between WT and PHPT1-KD rat lungs; CDKN1A was significantly decreased. Down: PCR verification of the RNA-seq results of TRPV5 and CDKN1A. **P** Western blot analysis of TRPV5, KCNN4, CDKN1A, p-Akt, p-SMAD2, p-SMAD3, p-TGF-β, RAC1, and p-EGFR protein expression compared with that of the β-tubulin loading control in WT and PHPT1-KD rat lungs with or without hypoxia exposure. **Q** Western blot result quantifications (n = 6). The relative expression of each protein was normalized to that of β-tubulin. The results were obtained from three independent experiments and are represented as the mean ± SD. KD, knockdown; WT, wild type; DEGs, differentially expressed genes; RNA-seq, RNA sequencing; PASMCs, human pulmonary artery smooth muscle cells. *p < 0.05 relative to the control. #p < 0.05 relative to the hypoxia model group. CW, control; CP, PHPT1-KD; MW, hypoxia model; MP, hypoxia model with PHPT1-KD.

confirmed using western blotting (Fig. 2A). The HPAH model was successfully established after continuously exposing the rats to a high altitude (5500 m) for 28 days. The rats displayed elevated mPAP and right ventricular systolic pressure (RVSP) compared with those in the control group (Fig. 2B and C), along with increases in the ratio of PAT/PET and RVAW and a decrease in tricuspid annular plane systolic excursion (TAPSE) (Fig. 2D and E). Under hypobaric hypoxia intervention, PHPT1-KD rats showed higher elevations in mPAP, RVSP, and RVAW and a decrease in PAT/ PET and TAPSE. Histological analysis using hematoxylin and eosin (H&E) staining revealed that the pulmonary tissue of PHPT1-KD rats exhibited destroyed alveolar structures in the lungs and thickened right ventricular (RV) walls in hearts compared with those in wild-type (WT) rats (Fig. 2F and G). Under hypobaric hypoxia intervention, PHPT1-KD rats

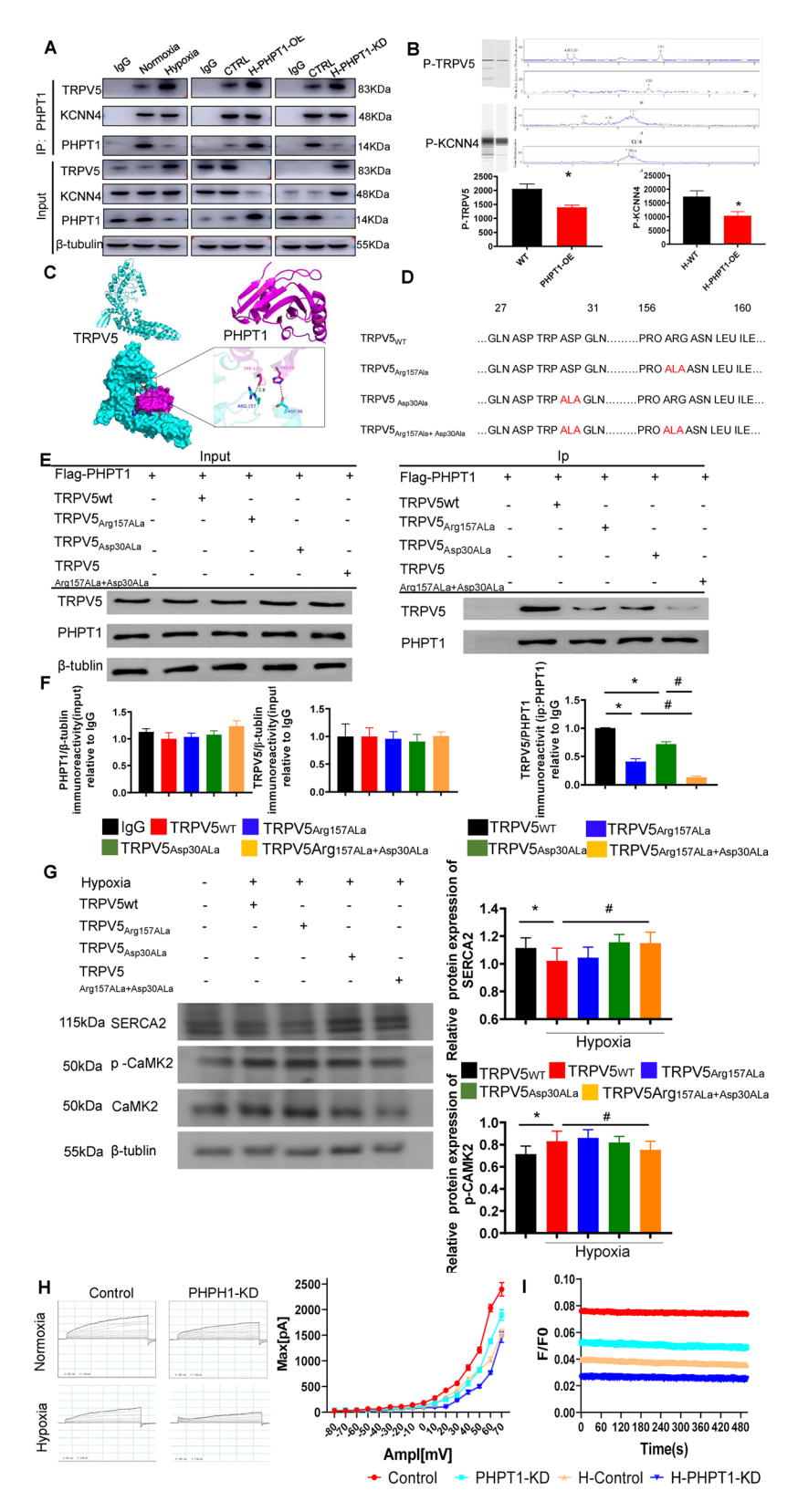


Fig. 4 (See legend on next page.)

Fig. 4 PHPT1 interacts with TRPV5, influencing spontaneous Ca^{2+} activity and Ca current. **A** Co-immunoprecipitation analysis of TRPV5-PHPT1. **B** Upper panel: TRPV5 and KCNN4 phosphorylation-related protein sample analysis. Lower panel: Protein phosphorylation result quantifications (n = 6). **C** PHPT1 interaction with TRPV5 predicted using HDOCK (http://hdock.phys.hust.edu.cn). Blue and pink represent TRPV5 and PHPT1, respectively, along with the 3D interaction image below. **D** Amino acid mutations in three TRPV5 variants. **E** PHPT1 expression and three TRPV5 mutations. Following the PHPT1 immunoprecipitation and TRPV5 protein mutations, TRPV5 and PHPT1 were assessed by immunoblotting. **F** Protein expression quantification (n = 6). **G** Left: Western blot results of changes in TRPV5 mutations on calcium pathway. The calcium pathway proteins include SERCA2, p -CaMK2, and CaMK2. The protein expression compared with that of the β-tubulin loading control. Right: Protein expression quantification. **H** Left panel: External membrane current activated by pulmonary artery smooth muscle cell depolarization. Right panel: I-V curve of the outgoing current. I Summary of the peak amplitudes as cytosolic Ca^{2+} changes detected by Fluo-4 fluorescence (F/F0).

presented with thickening and fibrosis of the alveolar septa and the decrease in the D/W ratio compared with that in WT rats (Fig. 2H and I). These findings indicate that PHPT1-knockdown induced cardiopulmonary injury and aggravated HAPH in hypobaric hypoxia.

PHPT1-KD results in cardiopulmonary injury by influencing spontaneous ion binding and the PI3K/Akt pathway

The hypoxia-induced phenotypic transformation of PASMCs in vitro was established to mimic in vivo conditions. To confirm the cause-effect relationship between PHPT1 and the phenotypic transformation of PASMCs, we established gene knockdown by transfecting PASMCs with adenovirus. The results showed that the proliferation of PASMCs was significantly increased under hypoxic conditions. PHPT1 knockdown led to further proliferation of hypoxia-treated PASMCs, as evidenced by CCK8 analysis (Fig. 3A). Moreover, impedance results show that PHPT1 knockdown enhanced the hypoxia-induced proliferation of PASMCs (Fig. 3B). To explore the effects of PHPT1 on hPASMC migration, transwell migration and scratch wound assays were conducted. Cell migration was significantly increased after hypoxic stimulation for 48 h, and PHPT1 knockdown significantly increased migration (Fig. 3C). The wound closure levels in the scratch wound assay were consistent with the results of the trans-well migration assay (Fig. 3D). To identify the molecular pathways underlying PHPT1-induced lung injury during HAPH, RNA sequencing (RNA-seq) analysis was performed on lung tissue from WT and PHPT1-KD rats after 4 weeks of high-altitude exposure. We screened 652 DEGs between the PHPT1-KD (MP) and WT (MW) model groups for analysis (Fig. 3E and Table S4). Furthermore, a principal coordinate analysis (PCoA) plot demonstrated distinct clusters among CW, CP, MW and MP over the first two dimensions (Fig. 3F), Gene ontology analysis of the DEGs among the four groups related to biological process(yellow), molecular function(pink) and cellular component(green) (Fig. 3G). Kyoto Encyclopedia of Genes and Genomes (KEGG) pathway analysis of the DEGs among the four groups related to environmental information processing(yellow), organismal systems(pink) and human disease(purple) (Fig. 3H). The significant DEmRNAs among the four groups were visualized in a heat map shown in Fig. 3I and verified by PCR (Fig. 3P). The top 20 genes with maximum abundance of MW/MP were shown in green/red (Fig. 3J). The GSEA results showed that the DEGs were mainly involved in the activation of Oxidative phosphorylation, proteasome, disease, DNA replication immune response, pentose phosphate pathway and so on. Gene ontology analysis of the DEGs between MP and MW revealed the enrichment of terms related to ion binding, especially Ca²⁺ binding and protein kinase activity. Kyoto Encyclopedia of Genes and Genomes (KEGG) pathway analysis confirmed the enrichment of pathways related to the PI3K/Akt signaling pathway (Fig. 3N). Among the top DEGs, TRPV5 were significantly upregulated in PHPT1-KD lung tissues (Fig. 3M). Among the top DEGs, CDKN1A were significantly downregulated in PHPT1-KD lung tissues (Fig. 3O). Additionally, we analyzed TRPV5 expression and possible signaling using western blotting. TRPV5, KCNN4, CDKN1A, p-Akt, p-SMAD2, p-SMAD3, p-TGF-β, RAC1, and p-EGFR expression was activated in the lungs of the HPAH group. The expression of TRPV5, KCNN4, p-Akt, p-SMAD2, p-SMAD3, p-TGF-β, RAC1, and p-EGFR was further upregulated in PHPT1-KD lungs under hypobaric hypoxia intervention (Fig. 3P and Q). These findings suggested that PHPT1-knockdown-induced lung injury was impaired due to spontaneous ion binding and disrupted expression of core proteins involved in PI3K/ Akt pathway.

PHPT1 interacts with TRPV5 and KCNN4, influencing spontaneous Ca²⁺ events and Ca current

TRPV5 and KCNN4 have been identified as PHPT1 substrates. Therefore, we confirmed a direct association among PHPT1, TRPV5, and KCNN4 using co-immuno-precipitation (Co-IP) assays. In contrast to the increased expression of TRPV5 and KCNN4 in the hypoxia and PHPT1-KD groups, their protein expression was reduced in the PHPT1-OE group, as indicated by immunoprecipitation (IP). Furthermore, the interaction between PHPT1 and TRPV5 or KCNN4 showed no obvious differences among the hypoxia, PHPT1-KD, or PHPT1-OE groups, as shown by IP (Fig. 4A). Next, we determined TRPV5 and KCNN4 phosphorylation using nanoproteomic analysis. The results revealed that PHPT1 downregulated the expression of phosphorylated TRPV5 and KCNN4 (Fig. 4B). Subsequently, we performed mutation

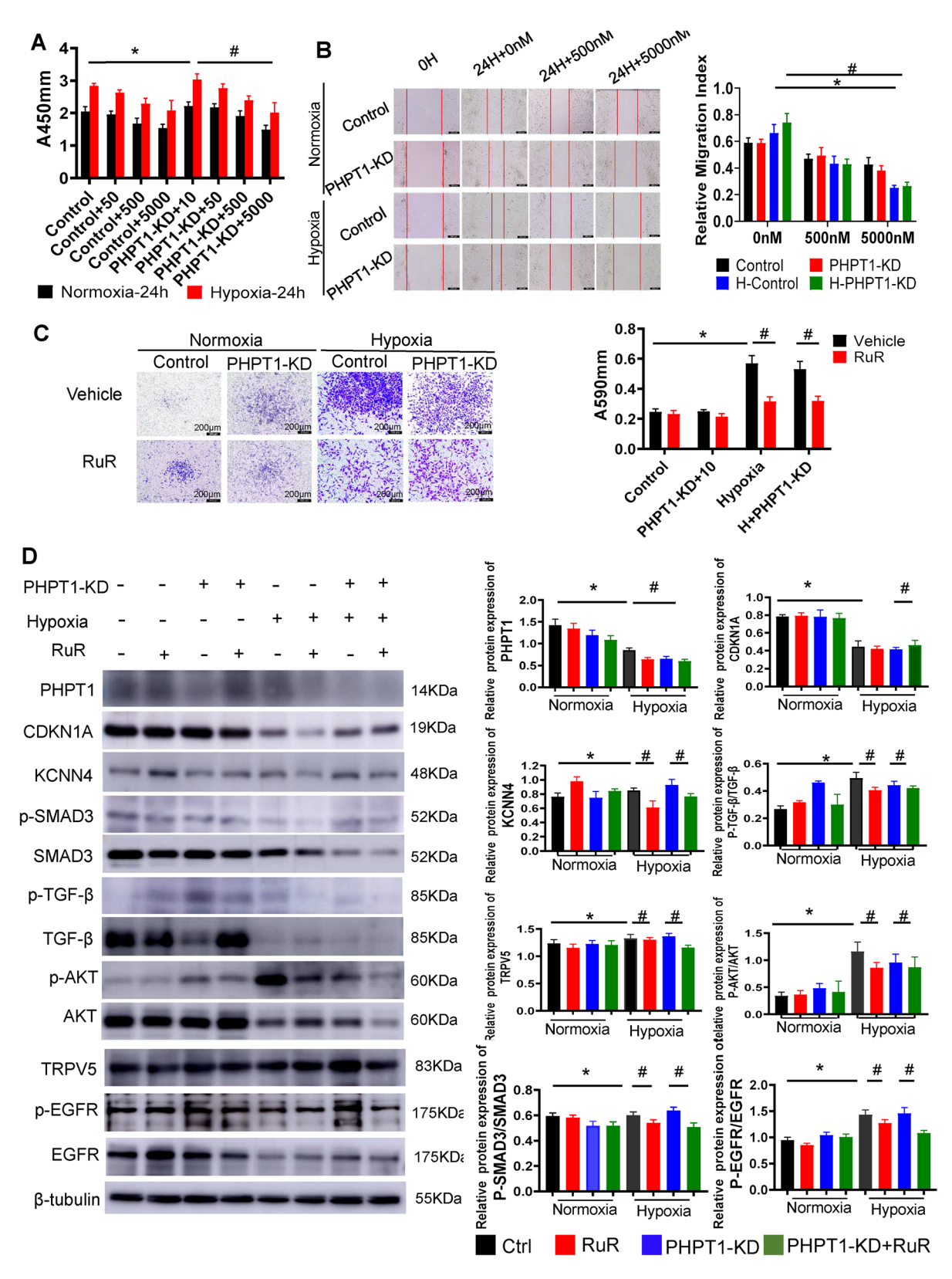


Fig. 5 (See legend on next page.)

Fig. 5 TRPV5 inhibition suppresses PASMC proliferation and migration. **A** PASMCs were treated with RuR (0–5000 nmol/L) for 24 h, then assessed using a cell counting kit-8 under normoxic or hypoxic (1 % O_2) conditions with or without PHPT1-KD. The absorbance was measured at 450 nm (n = 6). **B** Left panel: PASMCs treated with RuR (0–5000 nmol/L) and exposed to normoxic or hypoxic conditions with or without PHPT1-KD for 48 h. Representative images of the wound closure area. Right panel: Wound closure area quantification (n = 6). **C** PASMCs were seeded into the upper chambers of Transwell plates, treated with RuR, and exposed to normoxic or hypoxic conditions with or without PHPT1-KD. Representative images of migrated cells. **D** Left panel: western blot analysis of TRPV5, KCNN4, CDKN1A, p-Akt, p-SMAD2, p-SMAD3, p-TGFβ, RAC1, and p-EGFR protein expression compared with that of the β-tubulin loading control in WT and PHPT1-KD PASMCs treated with RuR for 24 h. Right panel: Quantification of western blot results.

and IP experiments. To explore the regulatory mechanisms of PHPT1, we used the HDOCK server to predict how the Arg 157 and Asp 30 residues of TRPV5 interact with PHPT1 (Fig. 4C). We constructed two mutant variants by individually substituting the two residues with alanine (Arg157Ala, Asp30Ala), and a third variant by mutating both residues with alanine simultaneously (Arg157Ala+Asp30Ala) (Fig. 4D). Co-precipitation of TRPV5 (WT) and the three mutant variants revealed that the Arg157Ala and Asp30Ala mutations partially impaired interaction between TRPV5 and PHPT1. The near disruption of contact occurred when both residues were mutated (Fig. 4E and F). TRPV5 acts as a transient receptor potential cation channel and an intermediateconductance Ca²⁺-activated potassium channel. The hypoxia group showed increased phosphorylation of CaMK2 and downregulated SERCA2. Furthermore, the TRPV5 mutation groups showed lower levels of phosphorylation of CaMK2 and higher levels of SERCA2 (Fig. 4G and H). To determine the Ca channel currents, we used the whole-cell patch clamp method. The Ca current recorded in PHPT1-KD cells was lower than that in untransfected cells (Fig. 4G). Additionally, the results of the Ca imaging of PASMCs showed spontaneous calcium activity (Fig. 4H). Meanwhile, the fluorescence intensity in PHPT1-KD cells was lower than that in untransfected ones (Fig. 4I). These findings suggest that PHPT1 interacted with TRPV5 and maintained the Ca2+-activated potassium channel.

Inhibiting TRPV5 and PI3K suppresses PASMC proliferation through PHPT1 silencing

To investigate whether TRPV5 and PI3K/Akt pathways mediate the alterations in PASMC phenotype and HPAH development, hypoxia and PHPT1 silencing-induced PASMCs were treated with RuR, a small molecule widely used to inhibit TRPV5, and AS252424, a PI3K/AKT pathway inhibitor. Relative to the hypoxia and PHPT1-KD groups, treatment with RuR or AS252424 significantly reduced the proliferative activity of PASMCs, as shown by CCK8 analysis (Figs. 5A and 6A). Cell migration was significantly increased in the hypoxia and PHPT1-KD groups, whereas TRPV5 and PI3K blockade by RuR and AS252424 attenuated the increases in migration (Figs. 5B and 6B). The wound closure levels in the scratch wound assay were consistent with the results of the transwell migration assay (Figs. 5C and 6C). RuR treatment

significantly suppressed the expression of TRPV5, KCNN4, p-Akt, p-SMAD3, p-TGF-β, and p-EGFR and upregulated that of CDKN1A (Fig. 5D). Treatment with AS252424 significantly downregulated the expression of p-Akt, p-SMAD3, and p-TGF-β, and augmented the expression of CDKN1A but not that of TRPV5, KCNN4, or p-EGFR (Fig. 6D). In summary, our findings indicated that TRPV5 and PI3K dysregulation downstream effects of PHPT1 inhibition and impaired PASMC function.

PHPT1-OE improves cardiopulmonary function and alleviates HAPH in hypobaric hypoxia

To examine whether PHPT1 overexpression ameliorates cardiopulmonary function in HAPH, we used CRISPR/ Cas9 technology to generate PHPT1 knock-in rats. The protein overexpression of PHPT1 in PHPT1-OE rats was confirmed using western blotting (Fig. 7A and S2). The HAPH model was successfully established after continuously exposing the rats to high-altitude conditions (5500 m) for 28 days. The rats exhibited elevated mPAP and RVSP, as well as reduced PAT/PET and TAPSE, compared with those in the control group. Under hypobaric hypoxia intervention, PHPT1-OE rats displayed significantly decreased RVSP and mPAP, accompanied by elevated PAT/PET and TAPSE (Fig. 7B and C). Histological analysis using H&E staining showed that the pulmonary tissue of PHPT1-OE rats had a superior lung alveolar structure and thinner RV walls in hearts compared with those of WT rats exposed to hypoxia (Fig. 7D and E). Under hypobaric hypoxia conditions, PHPT1-OE rats showed a significantly reduced D/W ratio and an attenuated MWT increase compared with those in WT rats (Fig. 7F). Overall, our results suggest that overexpression of PHPT1 alleviated HAPH and improved cardiopulmonary function in vivo.

PHPT1 overexpression inhibits PASMC proliferation/ migration and restores TRPV5 and p-Akt/p-SMAD3/p-TGF-β expression under hypoxic conditions

Further CCK8 and impledance experiments were conducted to assess the properties of PASMCs in PHPT1-OE groups. hPASMC proliferation significantly increased under hypoxic conditions, whereas PHPT1 overexpression inhibited hPASMC proliferation (Fig. 8A–C). Cell migration was significantly enhanced after hypoxic stimulation for 24 h. In contrast, PHPT1 overexpression attenuated the elevation in migration (Fig. 8D).

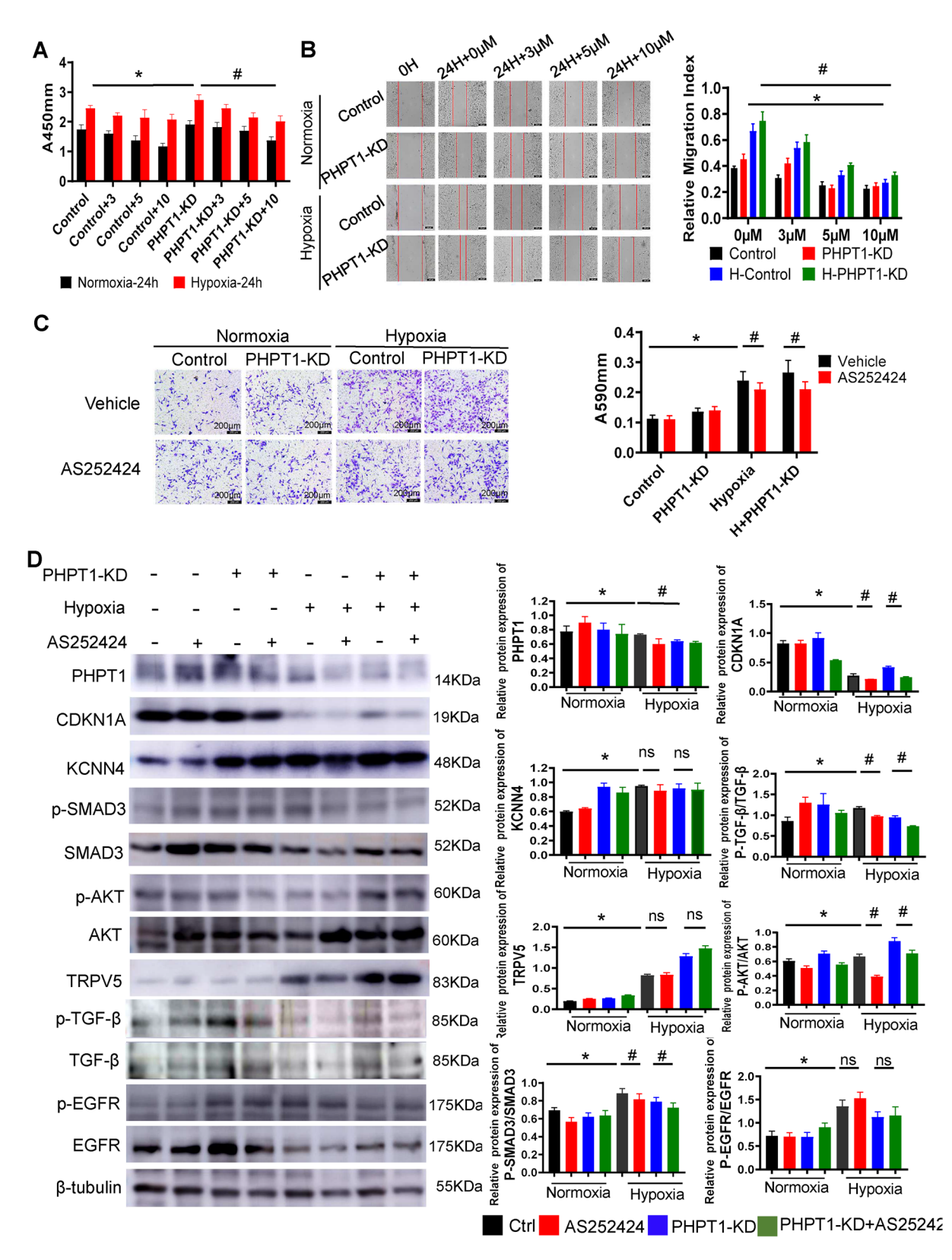


Fig. 6 (See legend on next page.)

Fig. 6 Inhibition of PI3K suppresses the proliferation and migration of PASMCs. **A** PASMCs were treated with AS252424 (0–10 μmol/L) for 24 h and assessed using cell counting kit-8 under normoxic or hypoxic conditions with or without PHPT1-KD, and absorbance was measured at 450 nm (n = 6). **B** Left panel: PASMCs were treated with AS252424 (0–10 μmol/L) and exposed to normoxic or hypoxic conditions with or without PHPT1-KD for 48 h. Representative images of the wound closure area. Right panel: Quantification of the wound closure area (n = 6). **C** PASMCs were seeded into the upper chambers of transwell plates, treated with AS252424, and exposed to normoxic or hypoxic conditions with or without PHPT1-KD for 48 h. Representative images of migrated cells are shown. **D** Left panel: Western blot analysis of TRPV5, KCNN4, CDKN1A, p-Akt, p-SMAD2, p-SMAD3, p-TGFβ, RAC1, and p-EGFR protein expression compared with that of the β-tubulin loading control in WT and PHPT1-KD PASMCs treated with AS252424 for 24 h. Right panel: Western blot result quantifications. PASMCs, pulmonary artery smooth muscle cells. *p < 0.05 relative to the control. #p < 0.05 relative to the hypoxia with the PHPT1-KD group.

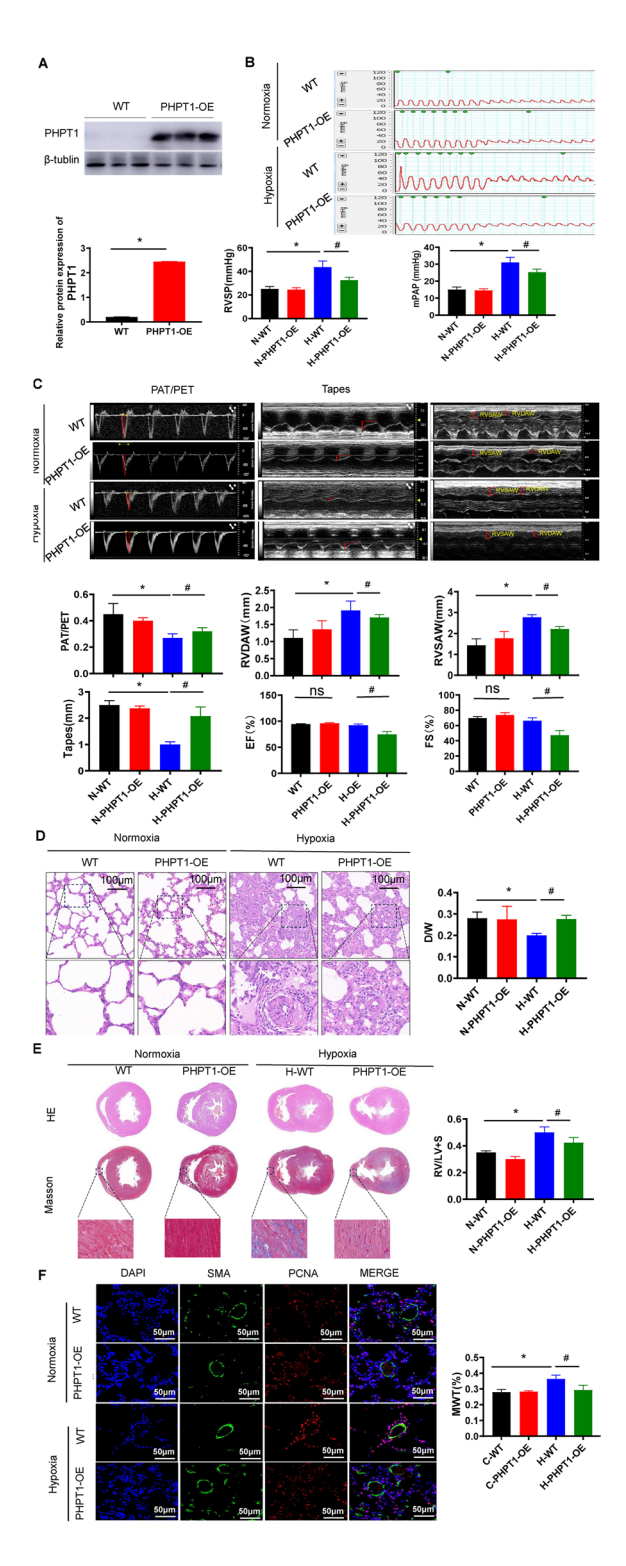
The wound closure levels in the scratch wound assay were consistent with the results of the transwell migration assay (Fig. 8E). Moreover, the Ca current recorded in PASMCs was significantly decreased under hypoxic conditions, but this effect was mitigated by PHPT1 overexpression. Ca imaging of PASMCs demonstrated spontaneous calcium activity. In addition, fluorescence intensity significantly decreased under hypoxic conditions. However, the overexpression of PHPT1 significantly inhibited this decrease (Fig. 8F and 7G). The expression of TRPV5, KCNN4, CDKN1A, p-Akt, p-SMAD2, p-SMAD3, p-TGF-β, RAC1, and p-EGFR were upregulated in the hypoxia group. By contrast, PHPT1-OE markedly downregulated the expression of these signaling markers and correspondingly augmented the protein expression of CDKN1A (Fig. 8H and I). Moreover, PHPT1 may be a promising therapeutic target for HAPH treatment by maintaining TRPV5/p-Akt protein expression and inhibiting uncontrolled PASMC proliferation.

Discussion

Some studies have described PHPT1's implication in lung cancer pathogenesis. For instance, study revealed that PHPT1 expression was significantly increased in the lung tissue of patients with lung cancer [11]. Furthermore, PHPT1 was not only expressed in the cytoplasm but also in lung cancer cell nuclei [12]. PHPT1 protein overexpression in the lung cancer tissue is consistent with previous PHPT1 mRNA expression results, which positively correlate with lung cancer stage and lymph node metastasis [13]. PHPT1 is reportedly likely functionally related to cell migration in lung cancer cells [14]. Additionally, in highly metastatic lung cancer CL1-5 cells, PHPT1 knockdown inhibited migration and invasion in vitro, although it did not alter the cell proliferation rate [15]. Proteome analysis elucidated different protein expression profiles, suggesting potential PHPT1 involvement in cytoskeletal recombination, which was further confirmed by F-actin filament staining [16]; it is closely related to lamellar pseudopodium formation, corresponding to an important cell movement structure, which considerably affects the biological functions of cell movement, including tumor cell metastasis [17]. Beyond lung cancer, PHPT1 is also reportedly functionally related to hepatic stellate cell migration in liver fibrosis [18]. The HAPH-related role of PHPT1 in PASMCs closely resembles its recently described functions in human cancers [19]. Herein, we uncovered a previously unrecognized role of PHPT1 in high-altitude-induced pulmonary hypertension as well as cardiac hypertrophy and dysfunction. We demonstrated that PHPT1 dysfunction upsets the balance between PASMC growth, death, and migration ability, favoring increased vasculature muscularization.

However, the underlying reason for the inhibited PHPT1 expression and activity in hypoxia-induced PASMCs remains elusive. Bioinformatics tools predicted that the Ca²⁺ binding pathway might involve a potential PHPT1-binding transcription factor. In the present study, we identified a novel mechanism, in which PHPT1 inhibition impaired Ca2+ homeostasis by TRPV5 expression upregulation. Ca2+ signaling is involved in multiple cardiac diseases, including coronary heart disease, atrial fibrillation, atherosclerosis, and heart failure [20]. KCa3.1, a PHPT1 phosphatase substrate, is a potassiumdependent Ca2+ channel protein. Abnormal K+ channel involvement has been reportedly implicated in HAPH induction [21]. The β 1 group in KCa is important in vasoconstriction through the main mechanism of vascular tension increase, thereby increasing pulmonary blood vessel pressure [22]. KCa mRNA and protein expression levels are upregulated during hypoxia, with pulmonary artery wall thickening and increased pressure [23]. Furthermore, KCa3.1 and TRPV expression is associated with oxygen-glucose deprivation-induced astrogliosis

TRPV5 serves as an active Ca²⁺ reabsorption gate-keeper [25] and mediates Ca²⁺ influx into the cells as the first step in transepithelial Ca²⁺ transport [26]. The kinase domain of WNK lysine-deficient protein kinase 3 could reportedly increase TRPV5-mediated Ca²⁺ transport [27]. Previous studies revealed that KCa3.1 and TRPV5 are both PHPT1 substrates. PHPT1 directly regulates the TRPV5 plasma membrane (PM) channel through reversible histidine phosphorylation, and this regulation is biologically significant [28, 29]. Herein, we demonstrated that inhibiting PHPT1 significantly enhanced TRPV5 phosphorylation. PHPT1 is a 125-amino acid-containing human cytoplasmic protein, with residues at its active site identified as Lys21, Glu51, Tyr 52, His53, Arg78,



Tyr3, and Met95. This active site provides a suitable environment for phosphohistidine-containing substrate binding [30]. PHPT1 mutation at the dibasic amino acids at positions 53 or 102 reportedly induces histidine phosphatase activity loss in PHPT1 [31]. Recently, a salt bridge was identified between the R78 guanidinium moiety and the C-terminal carboxyl group on Y125, which is critical

Fig. 7 PHPT1 overexpression rescues pulmonary vascular remodeling and alleviates HAPH in hypobaric hypoxia rats. A Upper panel: Western blot analysis of PHPT1 protein expression in lung tissue. Tubulin was used as a loading control. Lower panel: Quantification of western blot analysis from the upper panel, **B** Left panel; RVSP and mPAP were determined using invasive hemodynamic measurements. Right panel: Quantification of mPAP and RVSP (n = 12) **C** PAT/PET and TAPSE were measured using echocardiography. **D** Left panel: Microscopic images of lung tissues stained with H&E. Right panel: Quantification of lung dry-to-wet ratio (n = 12). **E** Left panel: Images of heart tissues stained with H&E and Masson's staining. Right panel: Quantification of Heart RV to LV+IS ratio (n = 12). **F** Lung tissue sections were stained with antibodies against α -SMA and the cell proliferation marker PCNA. MWT was determined using histological analysis. RVSP, right ventricular systolic pressure: mPAP, mean pulmonary artery pressure: PAT/PET, pulmonary acceleration time; pulmonary ejection time; TAPSE, tricuspid annular plane systolic excursion; H&E, hematoxylin and eosin; RV to LV+IS ratio, right ventricular to left ventricular + interventricular septum ratio; PCNA, proliferating cell nuclear antigen. *p < 0.05 relative to the control. #p < 0.05 relative to the hypoxia model group.

for PHPT1 ligand binding [32]. Using HDOCK prediction, we analyzed the impact of His-89 and Trp-120 on PHPT1 binding with the Asp30 and Arg157 mutations of TRPV5. We observed that Co-IP prevented the interaction between PHPT1 and TRPV5. However, Asp30Ala and Arg157Ala partially impaired PHPT1 binding with TRPV5. Overall, these results demonstrate that PHPT1 downregulation leads to impaired phosphorylation at Asp30 and Arg157 in TRPV5 and PASMC, thereby contributing to pulmonary hypertension injury development. Therefore, our discoveries indicate that PHPT1 inhibition could upregulate TRPV5 activation and increase PASMC proliferation and migration. Likewise, deleting the TRPV5 gene in B cells results in dysfunctional spreading and contraction [33]. It was previously reported that TRPV5 acts as a transient receptor potential cation channel and an intermediate-conductance Ca2+-activated potassium channel mediated by NDPK-B and PHPT1 [34]. SERCA2, a sarcoplasmic reticulum Ca²⁺-ATPase pump, is a calcium pump protein that can mediate sarcoplasmic reticulum Ca²⁺ reuptake. Decreased SERCA2 activity has been detected in heart failure [35]. CaMK2, a Ca²⁺/calmodulin-dependent protein kinase II, has been reported to be involved in inflammation. High levels of CaMK2 expression and phosphorylation indicate heart failure [36]. Our findings verify that hypoxia enhanced the phosphorylation levels of CaMK2 as well as the downregulation of SERCA2, which is consistent with the findings of earlier research. As previously described, TRPV5 acts as a transient receptor potential cation channel and regulate calcium-mediated signaling [26]. In our study, TRPV5 mutation elevated CaMK2 phosphorylation, and downregulated SERCA2 in PASMC, as confirmed by western blotting, suggesting the important role of TRPV5 and its involvement in the regulation of calcium signaling as a downstream of PHPT1 in HAPH.

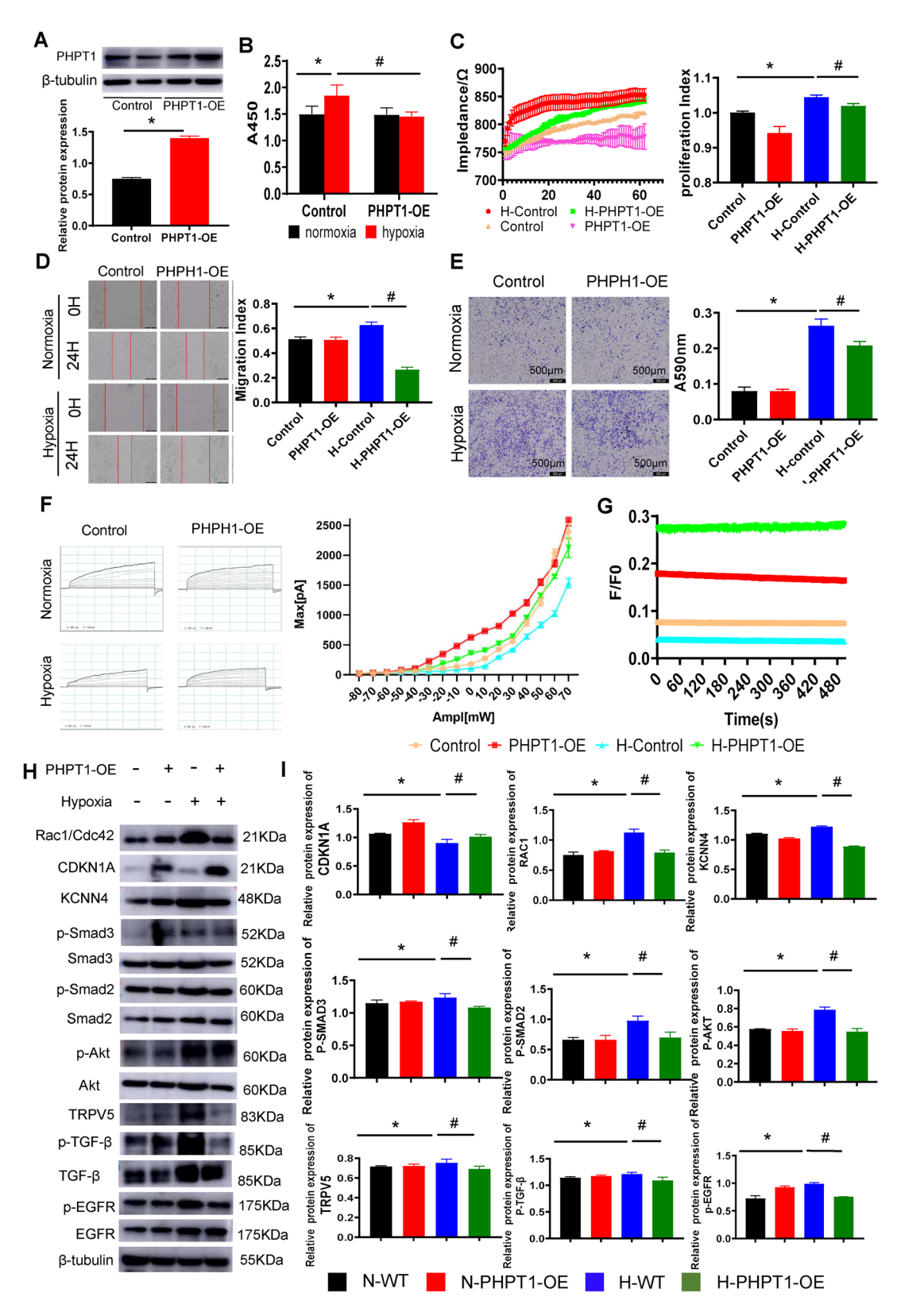


Fig. 8 (See legend on next page.)

Guo et al. Journal of Translational Medicine

(See figure on previous page.)

Fig. 8 Overexpression of PHPT1 mitigates the proliferation and migration of PASMCs and upregulates TRPV5/p-P13K/p-Akt expression under hypoxic conditions. **A** Western blot analysis of PHPT1 protein expression in PASMCs. Tubulin was used as a loading control. Quantification of western blot analysis from the upper panel. **B** Cell proliferation was determined using a cell counting kit-8 under normoxic or hypoxic conditions with or without PHPT1-OE, and absorbance was measured at 450 nm (n = 6). **C** Left panel: Cell proliferation was determined using impedance detection under normoxic or hypoxic conditions with or without PHPT1-OE. Right panel: Quantification of impedance analysis (n = 6). **D** Left panel: PASMCs were exposed to normoxic or hypoxic conditions with or without PHPT1-OE. Representative images of the wound closure area. Right panel: Quantification of the wound closure area (n = 6). **E** PASMCs were seeded into the upper chambers of Transwell plates and exposed to normoxic or hypoxic conditions with or without PHPT1-OE for 48 h. Representative images of migrated cells are shown. The migrated cells were quantified by detecting crystal violet levels (n = 6). **F** Left panel: External membrane current activated by depolarization of PASMCs. Right panel: The I-V curve of the outgoing current. **G** Summary of the peak amplitudes as cytosolic Ca²⁺ changes detected by Fluo-4 fluorescence (F/F0). **H** Western blot analysis of TRPV5, KCNN4, CDKN1A, p-Akt, p-SMAD2, p-SMAD3, p-TGF- β , RAC1, and p-EGFR protein expression compared with that of the β -tubulin loading control in WT and PHPT1-OE rat lungs with or without hypoxia exposure. **I** Western blot result quantifications. The relative expression of each protein was normalized to that of β -tubulin. The results were obtained from three independent experiments and are represented as the mean \pm SD. PASMCs, pulmonary artery smooth muscle cells; OE, overexpression. *p < 0.05 relative to the hypoxia model group.

In addition, RuR, a TRPV5 inhibitor, markedly alleviated PASMC proliferation by blocking TRPV5 expression through PHPT1 inhibition. In conclusion, these findings demonstrate that PHPT1 interacted with TRPV5, influencing Kca3.1 expression and impaired Ca²⁺ influx and PASMC function balance, thereby contributing to pulmonary hypertension injury development.

In this study, RNA-seq identified several genes highly enriched in the PI3K-Akt signaling pathway. PI3K is a widely expressed lipid kinase that phosphorylates phosphoinositides at the D-3 position of the inositol ring [37]. Growth factors and hormones trigger this phosphorylation event, which, in turn, coordinates cell growth, cycle entry, migration, and survival [38, 39]. Based on hematopoietic stem cell migration, PHPT1 was identified as a specific PI3Ky/Akt/Rac1 pathway mediator that regulates hepatic stellate cell migration, thereby participating in hepatic fibrosis. The dephosphorylation role of PHPT1 against the phosphorylated G protein GB dimers positioned PI3K as a G β subunit downstream effector [40]. However, another study described PHP14's dephosphorylation role against phosphorylated Akt in lung cancer cells. PI3K/AKT pathway inhibitor AS252424 treatment reduced PHPT1 overexpression-mediated Akt phosphorylation [41]. Consistent with these results, we noted that PHPT1 regulated the Akt downstream effector and its pathway. The difference in the role of PHPT1 against Akt phosphorylation might be dependent on cell phenotypeand the specific stimulus. However, near-complete but not complete disruption of contact resulted when Arg-157Ala and Asp30Ala, the two residues, were mutated, although other unidentified interactions could also exist.

To conclude, our findings mechanistically delineate that PHPT1 expression significantly decreased in high altitude-induced pulmonary hypertension. Pulmonary artery-specific PHPT1 deficiency was further aggravated in pulmonary artery-specific PHPT1 knockout transgenic rats. Mechanistically, PHPT1 deficiency upregulated TRPV5 expression to inactivate the PI3K/AKT/SMAD pathway, which resulted in pathological pulmonary vascular remodeling. (graphical abstract).

However, our study has some limitations. There were no human data or population validation on the effectiveness of PHPT1 for treating HAPH. In addition, near but not incomplete disruption of contact resulted when Arg-157Ala and Asp30Ala, the two residues were mutated. There may be a third or fourth interaction part not fully exhibited. There were no upstream regulators of PHPT1 validation on the effective of PHPT1 for treating HAPH. Further studies on the activated upstream regulators of PHPT1should be discussed. However, we proved that PHPT1 could be a therapeutic strategy for the treatment of HAPH. Thus, further studies on the specific therapeutic effects and safety of the drugs targeting PHPT1 in HAPH treatment might help to exploit the potential HAPH treatment approaches for clinical translation.

Conclusions

This study demonstrates that PHPT1 attenuates high altitude-induced pulmonary hypertension and cardiac hypertrophy by downregulating TRPV5/Akt signaling, and PHPT1 targeting could contribute to the development of novel HAPH treatment approaches.

Abbreviations

HAPH high altitude pulmonary hypertension pulmonary artery smooth muscle cells phosphohistidine phosphatase 1 right ventricular systolic pressure mean pulmonary artery pressure TAPSE tricuspid annular plane systolic excursion

PAT/PET pulmonary acceleration time/pulmonary ejection time

TRPV5 transient receptor potential cation channel subfamily V member 5

RVAW right ventricular anterior wall
RVHI Right ventricular hypertrophy index
PCNA proliferating cell nuclear antigen
DMEM Dulbecco's modified eagle medium

FBS foetal bovine serum MWT medial wall thickness

Supplementary Information

The online version contains supplementary material available at https://doi.org/10.1186/s12967-025-06980-8.

Supplementary Material 1.

Supplementary Material 2.

Acknowledgements

Not applicable.

Author contributions

GG, ZMX and XX performed the experiments, analyzed, interpreted the data and wrote the manuscript. LX, SYY and LHL helped to perform the experiments and conducted the data analyses. CLT revised the work for important intellectual conte. YYM and LCL conceived, designed this study, edited and revised the manuscript. All authors read and approved the final manuscript.

Funding

This work was supported by the National Natural Science Foundation of China (Grant No.82130062, 82101966) and the Talent Project of the Chinese PLA general Hospital.

Data availability

The datasets used and/or analyzed during the current study are available from the corresponding author on reasonable request.

Declarations

Ethics approval and consent to participate

The studies using human blood samples was approved by the Ethics Committee of PLA General Hospital. Animal experiments were approved by the Animal Ethical and Welfare Committee of the PLA General Hospital and were performed according to the guidelines for the care and use of laboratory animals.

Consent for publication

All authors approved the manuscript and gave their consent for submission and publication.

Competing interests

The authors have declared that no conflict of interest exists.

Author details

¹Medical Innovation Research Division of the Chinese PLA General Hospital, Beijing 100853, China

²Graduate School, The Chinese PLA General Hospital, Beijing 100853, China

³National Clinical Research Center for Geriatric Diseases, The Chinese PLA General Hospital, Beijing 100853, China

Received: 9 June 2025 / Accepted: 6 August 2025 Published online: 28 August 2025

References

- Ulloa NA, Cook J. Altitude-induced pulmonary hypertension. Treasure Island (FL): StatPearls Publishing; 2024.
- Dunham-Snary KJ, Wu D, Sykes EA, Thakrar A, Parlow LRG, Mewburn JD, et al. Hypoxic pulmonary vasoconstriction: from molecular mechanisms to medicine. Chest. 2017;151:181–92.
- Stenmark KR, Orton EC, Reeves JT, Voelkel NF, Crouch EC, Parks WC, et al. Vascular remodeling in neonatal pulmonary hypertension. Role of the smooth muscle cell. Chest. 1988;93:1275-133S.
- Li T, Liu B, Li NS, Luo XJ, Peng JW, Peng J. Vascular peroxidase 1 promotes phenotypic transformation of pulmonary artery smooth muscle cells via ERK pathway in hypoxia-induced pulmonary hypertensive rats. Life Sci. 2022;307:120910.
- 5. Barford D. Protein phosphatases. Curr Opin Struct Biol. 1995;5:728–34.
- Xu X, Li H, Wei Q, Li X, Shen Y, Guo G, et al. Novel targets in a high-altitude pulmonary hypertension rat model based on RNA-seq and proteomics. Front Med (Lausanne). 2021;8:742436.

- Zhang XQ, Sundh UB, Jansson L, Zetterqvist O, Ek P. Immunohistochemical localization of phosphohistidine phosphatase PHPT1 in mouse and human tissues. Ups J Med Sci. 2009;114:65–72.
- Xu A, Li Y, Zhao W, Hou F, Li X, Sun L, et al. PHP14 regulates hepatic stellate cells migration in liver fibrosis via mediating TGF-β1 signaling to PI3Kγ/AKT/ Rac1 pathway. J Mol Med (Berl). 2018;96:119–33.
- Zhang N, Liao Y, Lv W, Zhu S, Qiu Y, Chen N, et al. FBXO32 targets PHPT1 for ubiquitination to regulate the growth of EGFR mutant lung cancer. Cell Oncol (Dordr). 2022;45:293–307.
- Liu C, Chen X, Guo G, Xu X, Li X, Wei Q, et al. Effects of intermittent normoxia on chronic hypoxic pulmonary hypertension and right ventricular hypertrophy in rats. High Alt Med Biol. 2021;22:184–92.
- Ji L, Su S, Xin M, Zhang Z, Nan X, Li Z, et al. Luteolin ameliorates hypoxiainduced pulmonary hypertension via regulating HIF-2α-Arg-NO axis and PI3K-AKT-eNOS-NO signaling pathway. Phytomedicine. 2022;104:154329.
- Shen H, Yang P, Liu Q, Tian Y. Nuclear expression and clinical significance of phosphohistidine phosphatase 1 in clear-cell renal cell carcinoma. J Int Med Res. 2015;43:747–57.
- 13. Xu AJ, Xia XH, Du ST, Gu JC. Clinical significance of PHPT1 protein expression in lung cancer. Chin Med J (Engl). 2010;123:3247–51.
- Xu A, Li X, Wu S, Lv T, Jin Q, Sun L, et al. Knockdown of 14-kDa phosphohistidine phosphatase expression suppresses lung cancer cell growth in vivo possibly through inhibition of NF-κB signaling pathway. Neoplasma. 2016;63:540–7.
- Xu A, Hao J, Zhang Z, Tian T, Jiang S, Hao J, et al. 14-kDa phosphohistidine phosphatase and its role in human lung cancer cell migration and invasion. Lung Cancer. 2010;67:48–56.
- Demirci EK, Demirci T, Linder P, Trzewik J, GierKDwski JR, Gossmann M, et al. rhAPC reduces the endothelial cell permeability via a decrease of contractile tensions induced by endothelial cells. J Biosci Bioeng. 2012;114:212–9.
- Srivastava S, Li Z, Soomro I, Sun Y, Wang J, Bao L, et al. Regulation of KATP channel trafficking in pancreatic β-cells by protein histidine phosphorylation. Diabetes. 2018;67:849–60.
- Xu A, Zhou J, Li Y, Qiao L, Jin C, Chen W, et al. 14-kDa phosphohistidine phosphatase is a potential therapeutic target for liver fibrosis. Am J Physiol Gastrointest Liver Physiol. 2021;320:G351–65.
- Ahmed SIY, Ibrahim ME, Khalil EAG. High altitude and pre-eclampsia: adaptation or protection. Med Hypotheses. 2017;104:128–32.
- Nan J, Li J, Lin Y, Saif Ur Rahman M, Li Z, Zhu L. The interplay between mitochondria and store-operated Ca2+ entry: emerging insights into cardiac diseases. J Cell Mol Med. 2021;25:9496–512.
- Wandall-Frostholm C, Skaarup LM, Sadda V, Nielsen G, Hedegaard ER, Mogensen S, et al. Pulmonary hypertension in wild type mice and animals with genetic deficit in KCa2.3 and KCa3.1 channels. PLoS One. 2014;9:e97687.
- Barnes EA, Lee L, Barnes SL, Brenner R, Alvira CM, Cornfield DN. β1-Subunit of the calcium-sensitive potassium channel modulates the pulmonary vascular smooth muscle cell response to hypoxia. Am J Physiol Lung Cell Mol Physiol. 2018;315:L265–75.
- 23. Guo S, Shen Y, He G, Wang T, Xu D, Wen F. Involvement of Ca2+-activated K+ channel 31 in hypoxia-induced pulmonary arterial hypertension and therapeutic effects of TRAM-34 in rats. Biosci Rep. 2017;37:BSR20170763.
- Yi M, Wei T, Wang Y, Lu Q, Chen G, Gao X, et al. The potassium channel KCa3.1 constitutes a pharmacological target for astrogliosis associated with ischemia stroke. J Neuroinflammation. 2017;14:203.
- Zhang W, Na T, Peng JB. WNK3 positively regulates epithelial calcium channels TRPV5 and TRPV6 via a kinase-dependent pathway. Am J Physiol Renal Physiol. 2008;295:F1472-84.
- Zhong G, Long H, Chen F, Yu Y. Oxoglaucine mediates Ca2+ influx and activates autophagy to alleviate osteoarthritis through the TRPV5/calmodulin/ CAMK-II pathway. Br J Pharmacol. 2021;178:2931–47.
- 27. Na T, Peng JB. TRPV5: a Ca(2+) channel for the fine-tuning of Ca(2+) reabsorption. Handb Exp Pharmacol. 2014;222:321–57.
- Srivastava S, Zhdanova O, Di L, Li Z, Albaqumi M, Wulff H, et al. Protein histidine phosphatase 1 negatively regulates CD4T cells by inhibiting the K+ channel KCa3.1. Proc Natl Acad Sci U S A. 2008;105:14442–6.
- Cai X, Srivastava S, Surindran S, Li Z, SKDLnik EY. Regulation of the epithelial Ca²⁺ channel TRPV5 by reversible histidine phosphorylation mediated by NDPK-B and PHPT1. Mol Biol Cell. 2014;25:1244–50.

- 30. Busam RD, Thorsell AG, Flores A, Hammarström M, Persson C, Hallberg BM. First structure of a eukaryotic phosphohistidine phosphatase. J Biol Chem. 2006;281:33830–4.
- 31. Ma R, Kanders E, Sundh UB, Geng M, Ek P, Zetterqvist O, et al. Mutational study of human phosphohistidine phosphatase: effect on enzymatic activity. Biochem Biophys Res Commun. 2005;337:887–91.
- 32. Zavala E, Dansereau S, Burke MJ, Lipchock JM, Maschietto F, Batista V, et al. A salt bridge of the C-terminal carboxyl group regulates PHPT1 substrate affinity and catalytic activity. Protein Sci. 2024;33(6): e5009.
- Mahtani T, Sheth H, Smith LK, Benedict L, Brecier A, Ghasemlou N, et al. The ion channel TRPV5 regulates B-cell signaling and activation. Front Immunol. 2024;15:1386719.
- Cai X, Srivastava S, Surindran S, Li Z, Skolnik EY. Regulation of the epithelial Ca2+ channel TRPV5 by reversible histidine phosphorylation mediated by NDPK-B and PHPT1. Mol Biol Cell. 2014;25:1244–50.
- Zhang T, Brown JH. Role of Ca2+/calmodulin-dependent protein kinase II in cardiac hypertrophy and heart failure. Cardiovasc Res. 2004;63:476–86.
- 36. Fischer TH, Eiringhaus J, Dybkova N, Förster A, Herting J, Kleinwächter A, et al. Ca(2+)/calmodulin-dependent protein kinase II equally induces sarcoplasmic

- reticulum Ca(2+) leak in human ischaemic and dilated cardiomyopathy. Eur J Heart Fail. 2014;16:1292–300.
- 37. Cantley LC. The phosphoinositide 3-kinase pathway. Science. 2002;296:1655–7.
- 38. Palmer TD, Ashby WJ, Lewis JD, Zijlstra A. Targeting tumor cell motility to prevent metastasis. Adv Drug Deliv Rev. 2011;63:568–81.
- 39. Neri LM, Borgatti P, Capitani S, Martelli AM. The nuclear phosphoinositide 3-kinase/AKT pathway: a new second messenger system. Biochim Biophys Acta. 2002;1584:73–80.
- 40. Mäurer A, Wieland T, Meissl F, Niroomand F, Mehringer R, Krieglstein J, et al. The beta-subunit of G proteins is a substrate of protein histidine phosphatase. Biochem Biophys Res Commun. 2005;334:1115–20.
- Xu C, Chen S, Deng Y, Song J, Li J, Chen X, et al. Distinct roles of PI3Kδ and PI3Kγ in a toluene diisocyanate-induced murine asthma model. Toxicology. 2021;454:152747.